Reduced survival of lens epithelial cells in the αA-crystallin-knockout mouse

Jing Hua Xi[1], Fang Bai[1] and Usha P. Andley[1,2,*]

[1]Department of Ophthalmology and Visual Sciences, and [2]Department of Biochemistry and Molecular Biophysics, Washington University School of Medicine, St Louis, MO 63110, USA

*Author for correspondence (e-mail: andley@vision.wustl.edu)

Accepted 17 December 2002
Journal of Cell Science 116, 1073-1085 © 2003 The Company of Biologists Ltd
doi:10.1242/jcs.00325

Summary

αA-Crystallin (αA) is a molecular chaperone expressed preferentially in the lens. αA transcripts are first detected during the early stages of lens development and its synthesis continues as the lens grows throughout life. αA$^{-/-}$ mouse lenses are smaller than controls, and lens epithelial cells derived from these mice have diminished growth in culture. In the current work, we tested the hypothesis that αA prevents cell death at a specific stage of the cell cycle in vivo. Seven-day-old 129Sv (wild-type) and αA$^{-/-}$ mice were injected with 5-bromo-2′-deoxyuridine (BrdU) to label newly synthesized DNA in proliferating cells. To follow the fate of the labeled cells, wholemounts of the capsule epithelial explants were made at successive times after the BrdU pulse, and the labeling index was determined. Immunofluorescence and confocal microscopy showed that both wild-type and αA$^{-/-}$ cells had a 3-hour labeling index of 4.5% in the central region of the wholemount, indicating that the number of cells in S phase was the same. Twenty-four hours after the pulse, individual cells labeled with BrdU had divided and BrdU-labeled cells were detected in pairs. The 24-hour labeling index in the wild-type lens was 8.6%, but in the αA$^{-/-}$ lens it was significantly lower, suggesting that some of the cells failed to divide and/or that the daughter cells died during mitosis. TUNEL labeling was rarely detected in the wild-type lens, but was significant and always detected in pairs in the αA$^{-/-}$ wholemounts. Dual labeling with TUNEL and BrdU also suggested that the labeled cells were dying in pairs in the αA$^{-/-}$ lens epithelium. Immunolabeling of wholemounts with β-tubulin antibodies indicated that the anaphase spindle in a significant proportion of αA$^{-/-}$ cells was not well organized. Examination of the cellular distribution of αA in cultured lens epithelial cells showed that it was concentrated in the intercellular microtubules of cells undergoing cytokinesis. These data suggest that αA expression in vivo protects against cell death during mitosis in the lens epithelium, and the smaller size of the αA$^{-/-}$ lens may be due to a decrease in the net production of epithelial cells.

Key words: αA-Crystallin, Lens, Chaperone, Cell death

Introduction

α-Crystallin is the major component of vertebrate eye lenses and constitutes approximately a third of the lens fiber cell proteins (Horwitz, 2000). It is also expressed at lower levels in lens epithelial cells. α-Crystallin is a hetero-oligomeric complex of two closely related polypeptides, αA and αB, present in 3:1 stoichiometry in lens fibers. The two subunits have chaperone activity, and are members of the small heat shock protein (HSP) family of molecular chaperones (Horwitz, 1992; de Jong, 1993; Sax and Piatigorsky, 1994). αA and αB transcripts are detected during the early stages of lens development (Robinson and Overbeek, 1996), and a marked increase in expression of the proteins accompanies differentiation. Both have been detected in tissues outside the lens, but αA is more lens-specific than αB (Bhat and Nagineni, 1989; Srinivasan et al., 1992; Sax and Piatigorsky, 1994). αA and αB are important for lens transparency and refraction. However, their ability to prevent the aggregation of denaturing proteins in vitro suggests that they may act as a 'sink' for age-related denatured proteins in the lens (Horwitz, 2000). The enhanced resistance of cells expressing these proteins to stress conditions suggests that αA and αB have general in vivo cellular functions in addition to a role in maintaining lens transparency.

αA- and αB-knockout mice have been generated to understand the physiological functions of these proteins (Brady et al., 1997; Brady et al., 2001). Disruption of the αA gene causes early-onset cataract in mice characterized by a central opacity owing to formation of inclusion bodies comprising αB and HSP25. Lenses of αA$^{-/-}$ mice are significantly smaller than normal (Brady et al., 1997), and lens epithelial cells derived from αA$^{-/-}$ mice have a 50% slower growth rate in vitro (Andley et al., 1998). Disruption of the gene encoding αB does not result in altered lens morphology or transparency. However, lens epithelial cells derived from αB$^{-/-}$ mice demonstrate hyperproliferation and genomic instability (Andley et al., 2001). These findings suggest that αA and αB may be essential for optimal growth of lens epithelial cells.

The lens grows throughout life as fiber cells are added incrementally at the lens periphery without concomitant loss of any previously formed fibers (Kuszak et al., 2000). The lens epithelium also undergoes lifelong growth, but with significant zonal variation as a function of age. The central epithelium

comprises a broad cap that covers the anterior surface of the lens. The mitotic activity of central epithelial cells decreases with age (Mikulicich and Young, 1963). The peripheral region of the epithelium contains mitotically active cells throughout life. As more cells in this region divide, they force the migration of other cells towards the equator to occupy the differentiating meridional rows, where they elongate bidirectionally until they become secondary fibers. Cells of the meridional rows are terminally differentiated and post-mitotic. Cell division is also absent in the transitional zone just anterior to the meridional rows (Rafferty and Rafferty, 1981). Growth and survival factors that influence cell division in the lens have been extensively studied (Reddan, 1982; McAvoy and Chamberlain, 1989; Hyatt and Beebe, 1993; Ishizaki et al., 1993; Zelenka et al., 1997; Rakic et al., 1997; Singh et al., 2000). However, regulation of cell division in the lens is not fully understood.

Several observations suggest that molecular chaperones play important roles in cell growth and differentiation (Mehlen et al., 1997; Yokota et al., 1999). It has been reported that HSP70, HSP90 and the major eukaryotic cytoplasmic chaperone TRiC may participate in the quality control of proteins during the progression of the cell cycle (Yokota et al., 1999; Dunn et al., 2001). TRiC plays an important role in cell growth by assisting in the folding of tubulin and other proteins, and its expression is strongly upregulated during cell growth, especially from the G_1/S transition to early S phase (Yokota et al., 1999). Mutations in TRiC genes cause aberrant chromosome segregation (Dunn et al., 2001). Both HSP70 and HSP90 have been detected in centrosomes of mitotic cells (Wigley et al., 1999; Brown et al., 1996). The reported increase in expression of αB in mitotic fibroblasts and its transient expression in the nucleus during interphase suggests its association with the cell-cycle machinery (Bhat et al., 1999; Djabali et al., 1999). In addition, antibodies to phosphorylated αB recognize midbodies and centrosomes of dividing cells (Inaguma et al., 2001). It has been suggested that chaperones may play a role in quality control of proteins, particularly in the assembly of microtubules. Although the expression of αA has been shown to enhance the growth of lens epithelial cells (Andley et al., 1998), it is not known whether it directly affects the progression of cells through the cell cycle.

Recently, mutations in αA and αB genes have been shown to be associated with genetic disorders. In αA, substitution of arginine 116 by cysteine was found to be the cause of one form of autosomal dominant cataract (Litt et al., 1998). In αB, substitution of arginine 120 by glycine was found to be the cause of another autosomal dominant disease, desmin-related myopathy, and also caused cataract (Vicart et al., 1998). It is not yet known whether these mutations also affect lens epithelial cell growth in vivo.

We have demonstrated that primary lens epithelial cells derived from $\alpha A^{-/-}$ mice grow at a 50% slower rate than controls (Andley et al., 1998). $\alpha A^{-/-}$ lenses are significantly smaller than controls (Brady et al., 1997). These data suggested that αA might be necessary for lens epithelial cells to proliferate at a normal rate in vivo. αA protects against stress-induced apoptosis (Andley et al., 1998; Andley et al., 2000), and the lack of αA may increase lens epithelial cell death. We tested the hypothesis that αA prevents cell death at a specific stage of the cell cycle in vivo and that the smaller size of the αA-knockout mouse lens is owing to the reduced survival of lens epithelial cells. We labeled the newly synthesized DNA of proliferating lens cells with 5-bromo-2′-deoxyuridine (BrdU), and followed the BrdU-labeled cells as they progressed through the cell cycle. We show that $\alpha A^{-/-}$ lens cells died as pairs during mitosis. These studies suggest that αA plays an important role in the regulation of mitosis in vivo.

Materials and Methods

Animals

Wild-type and $\alpha A^{-/-}$ mice were used in this study. Wild-type mice were 129SvEv strain from the Taconic Laboratories. The $\alpha A^{-/-}$ mice were kindly provided by E. Wawrousek (National Eye Institute). Mice were inbred and 7-day-old animals were used in these studies. All animal protocols were in accordance with the institutional policy for conduct of animal research.

Labeling of lenses with BrdU

Mice were injected with BrdU intraperitoneally (0.1 ml of a 10 mM solution of BrdU in sterile PBS) between 9 AM and 10 AM and were sacrificed 1, 3, 8, 16, 24 hours or 2, 3, 5 days later. Previous studies in rodents showed that, with this dose of BrdU, blood levels peak by 2 hours after injection and decline substantially thereafter (deFazio et al., 1987). Whole lenses were dissected under a microscope. In a 7-day-old lens, blood vessels on the posterior side were used to identify the orientation of the lens. The lens was placed in tissue culture medium in a coated tissue culture dish (Falcon 3001, 35 mm). To obtain the capsule-epithelial wholemounts, the lens was placed posterior-side up, and the capsule was held with very sharp tweezers and pulled. An opening was made at the edge of the posterior capsule, and blunt tweezers were used to flatten the capsule on the culture dish.

BrdU detection

In preparation for BrdU antibody staining, wholemounts were fixed with ethanol/glycine/water (70:20:10, v/v), pH 2.0 and 0.5% Triton X-100 for 30 minutes, followed by washing three times for 5 minutes each with PBS. Tissues were stored at 4°C in PBS containing 0.02% sodium azide. To detect BrdU, wholemounts were treated with a monoclonal antibody from the BrdU labeling kit (Roche Biochemicals) at a dilution of 1:100 in 1% bovine serum albumin, 0.5% Tween-20 in PBS for 2 hours, washed extensively in several changes of PBS with gentle agitation, and exposed to $Alexa^{568}$-labeled goat anti-mouse IgG (Molecular Probes) at a concentration of 1:200 diluted in PBS-BSA-Tween for 2 hours. Tissues were washed three times in PBS. In these studies, the DNA-binding dye TOTO-1 (Molecular Probes) was also used to determine the total number of cells. After BrdU labeling, wholemounts were stained with a 1:10 000 dilution of TOTO-1 for 20 minutes. After washing, tissues were mounted on microscope slides and viewed. BrdU fluorescence was analyzed in the red channel (excitation 568 nm) of a Zeiss LSM 410 confocal microscope. TOTO-1 was detected in the green channel (excitation 488 nm). Since the wholemount is not always completely flat, immunofluorescence detection with confocal microscopy allowed serial optical sections with a high degree of sensitivity and 3D images were collapsed into 2D to eliminate optical artifacts. Wholemounts were sampled by collecting serial images through the lens epithelium in the central region and in the equatorial region.

Labeling index

To determine the labeling index in different regions of the lens epithelial wholemounts, tissues were first examined at 10× magnification. The central region of the wild-type epithelium was

identified by its lower degree of BrdU labeling (as compared with the germinative region), and the area of the central region was 700-800 μm^2. The germinative region near the periphery of the wholemount had an area of about 180 μm^2. In each wholemount, three 150 μm^2 fields of the central lens epithelial region were examined. BrdU-labeled nuclei were counted in each field, and the total number of nuclei was determined by counting the TOTO-1-stained nuclei in the same field. The Scion Image (Scion Corp) program was used to count the labeled nuclei. For each genotype, six lenses were used. The labeling index was determined by dividing the number of BrdU-labeled cells by the total number of cells, multiplied by 100. Statistical analysis was carried out using the Student's *t*-test.

In our studies, we compared the labeling index of the peripheral region of wild-type cells with αA$^{-/-}$ lens epithelial cells. Our data showed that a large amount of BrdU labeling was occurring in the germinative region of the epithelium of 7-day-old mouse lenses. The number of labeled pairs 24 hours after the BrdU pulse was so high that it was difficult to assess accurately whether they were members of a pair or not. Thus, the analysis of the number of BrdU-labeled cells present as pairs is restricted to the central region of the epithelium.

To follow daughter cells produced after mitosis of BrdU-labeled cells, we counted the number of pairs of BrdU-labeled nuclei in lens epithelial wholemounts at 1, 2, 3 or 5 days after labeling. The identification of cell pairs was carried out as described previously (Beebe and Masters, 1996). In these analyses, single-labeled cells at the edge of a field were not counted as a pair, because it is possible that these could be paired with a nucleus that was out of the field of view. BrdU-labeled cells were counted as members of a cell pair when their nuclei were contiguous or separated by one or two nuclear diameters, and when the staining pattern of their nuclei was identical. The staining pattern of some pairs of BrdU-labeled nuclei was uniformly bright, whereas others had faint or diffuse label or a characteristically punctate appearance. These differences may result from the availability of BrdU to cells in different phases of the cell cycle at the time of BrdU injection. Adjacent BrdU-labeled nuclei were only scored as pairs when both cells had the same labeling pattern.

The proportion of BrdU-labeled cells in pairs was determined at each interval after BrdU injection. In our data, we observed that cell pairs with identical BrdU staining patterns 5 days after labeling were separated by up to four nuclear diameters, either because of migration, or because the cells separating them had undergone cell division.

Analysis of cell death

TUNEL labeling was used to examine cell death in lens epithelial wholemounts from wild-type and αA$^{-/-}$ mouse lenses. Wholemounts were fixed in 4% para-formaldehyde, pH 7.4 for 30 minutes, permeabilized for 5 minutes in 0.1% Triton X-100/PBS at room temperature, and apoptotic nuclei were detected using a TUNEL-labeling reaction according to the manufacturer's instructions (Roche Biochemicals), as described previously (Andley et al., 1998). In explants prepared for double labeling with TUNEL and BrdU, the TUNEL reaction was carried out first, and then the tissues were treated according to the protocol described above for BrdU detection. Images were recorded on a confocal microscope. BrdU was detected in the red channel (568 nm excitation) and TUNEL in the green channel (488 nm excitation). In other experiments, TUNEL-labeled tissues were co-labeled with propidium iodide (PI) to visualize individual nuclei in the wholemount. TUNEL-labeling was detected in the green channel and PI labeling in the red channel of the confocal microscope.

Labeling of MIP

To examine the cross-sectional profiles of lens fiber cells of wild-type and αA$^{-/-}$ lens sections, tissues were treated with an antibody to MIP (Alpha Diagnostics International). Lenses were mounted in glycol methacrylate and 3 μm sections were cut in the equatorial plane. Non-specific binding was blocked by incubation in 10% normal goat serum for 30 minutes. To visualize the distribution of MIP, tissues were incubated overnight with a 1:100 dilution of a monoclonal antibody to MIP. An Alexa^{568}-conjugated goat anti-mouse IgG was used as a secondary antibody (1:200). Immunofluorescence and confocal microscopy were performed as described above.

Labeling of αA

To visualize αA in wholemounts of wild-type and αA$^{-/-}$ lenses, tissues were incubated overnight with a 1:50 dilution of a monoclonal antibody to bovine αA (a gift from P. Fitzgerald, University of California, Davis, CA). An Alexa^{568}-conjugated goat anti-mouse IgG was used as a secondary antibody. Wholemounts were mounted on slides and were viewed using a Zeiss LSM 410 confocal microscope equipped with an argon-krypton laser. To visualize αA in mitotic cells, lens epithelial cells were cultured from wild-type lenses, and primary cells were labeled with the αA antibody. αA was visualized by Alexa^{568}-conjugated goat anti-mouse IgG as the secondary antibody, and F-actin was visualized by fluorescein phalloidin (Molecular Probes).

Labeling of β-tubulin

To visualize microtubules in whole mounts of wild-type and αA$^{-/-}$ lenses, tissues were incubated overnight with a 1:100 dilution of a monoclonal antibody to bovine β-tubulin (Sigma). An Alexa^{568}-conjugated goat anti-mouse IgG was used as a secondary antibody. Wholemounts were labeled with TOTO-1 to visualize nuclei. Wholemounts were mounted on slides and were viewed using a Zeiss LSM 410 confocal microscope equipped with an argon-krypton laser. β-tubulin was visualized in the red channel of the confocal microscope (568 nm excitation). TOTO-1 was detected in the green channel (488 nm excitation).

In other studies, dual labeling of cells was carried out with αA and β-tubulin antibodies. Cells were first incubated with the αA antibody and the Alexa^{488}-conjugated goat anti-mouse IgG secondary antibody (488 nm excitation), fixed again and then treated with an antibody to β-tubulin and Alexa^{568}-conjugated secondary antibody (568 nm excitation). To visualize nuclei, the DNA-binding dye TOPRO-3 was used (647 nm excitation).

Growth rate

Wet weights of wild-type and αA$^{-/-}$ lenses were determined for 7-day-old mice. The neonate lens was too small to be weighed accurately, but changes in lens size were determined from the diameter, which could be precisely measured. The equatorial and axial diameters of the lens were determined by acquiring differential interference contrast images in the confocal microscope of 4 μm paraffin sections at daily intervals.

Results

αA was detected in cells of the wild-type lens epithelial wholemounts by immunofluorescence. Fig. 1A shows merged confocal images of αA immunofluorescence and TOTO-1-labeled nuclei in the wholemount of a wild-type lens epithelium. In these wholemount preparations, the brightest αA immunofluorescence was observed in the basal region (towards the capsule). In wholemounts prepared from the αA$^{-/-}$ lenses, αA immunofluorescence was undetectable (Fig. 1B).

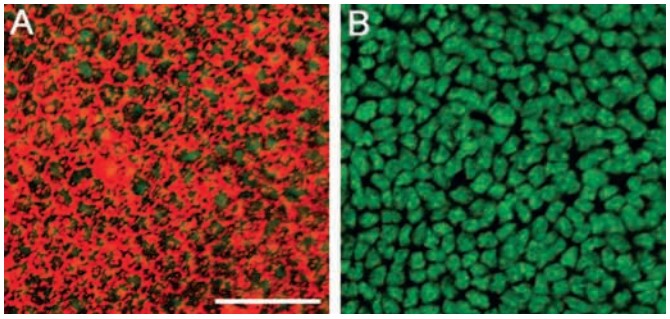

Fig. 1. Expression of αA in lens epithelial wholemounts by immunofluorescence. Wholemounts prepared from wild-type and $\alpha A^{-/-}$ lenses were stained with a monoclonal antibody to αA and an Alexa^{568}-labeled secondary antibody (red). The DNA-binding dye TOTO-1 (green) was used to stain the epithelial cell nuclei. (A) Merged confocal micrographs of αA and nuclei visualized in the wholemount of a wild-type mouse lens. (B) Lens epithelial wholemount from an $\alpha A^{-/-}$ mouse. No αA immunofluorescence was detected from the $\alpha A^{-/-}$ lens epithelial wholemount. Bar, 25 μM.

The wet weight of the wild-type 7-day-old lens was 1.50±0.4 mg, whereas that of the $\alpha A^{-/-}$ lens was 0.78±0.10 mg (n=6, P=0.004). We examined whether the 48% smaller lens was due to a decrease in the net production of epithelial cells or to smaller fiber cells size. We measured the proliferation index and apoptosis in the lens epithelial wholemount and recorded the cross-sectional area of secondary fiber cells.

αA expression has been shown to enhance lens epithelial growth in culture, but it is not known whether it affects proliferation in vivo. To test the hypothesis that αA expression plays a direct role in the regulation of the cell cycle by preventing cell death at a specific stage of the cell cycle, the newly synthesized DNA in proliferating cells was labeled in vivo. $\alpha A^{-/-}$ and control mice were injected with BrdU to label cells in the S phase, and the labeled cells were followed as their cell cycle progressed from the S to the G_2 and M phases, and after the completion of mitosis. Wholemounts of capsule epithelial explants were made, and labeled nuclei were detected with an antibody to BrdU. Three hours after BrdU injection, single, labeled nuclei were seen throughout the central epithelium of the wild-type lens (Fig. 2A-C). In the $\alpha A^{-/-}$ lenses, the majority of the BrdU-labeled nuclei also appeared as single labels, with distinct staining patterns (Fig. 2D-F). Labeling of the whole mounts with the DNA-binding dye TOTO-1 stained all nuclei, which could then be counted to determine the labeling index.

The labeling index 3 hours after the pulse was the same (4.5%) in wild-type and $\alpha A^{-/-}$ lens epithelial wholemounts (Fig. 2G). This observation indicates that the number of cells in the S phase was the same in both genotypes.

Other mice were killed the next day, by which time the individual cells labeled in S phase had divided to give pairs of

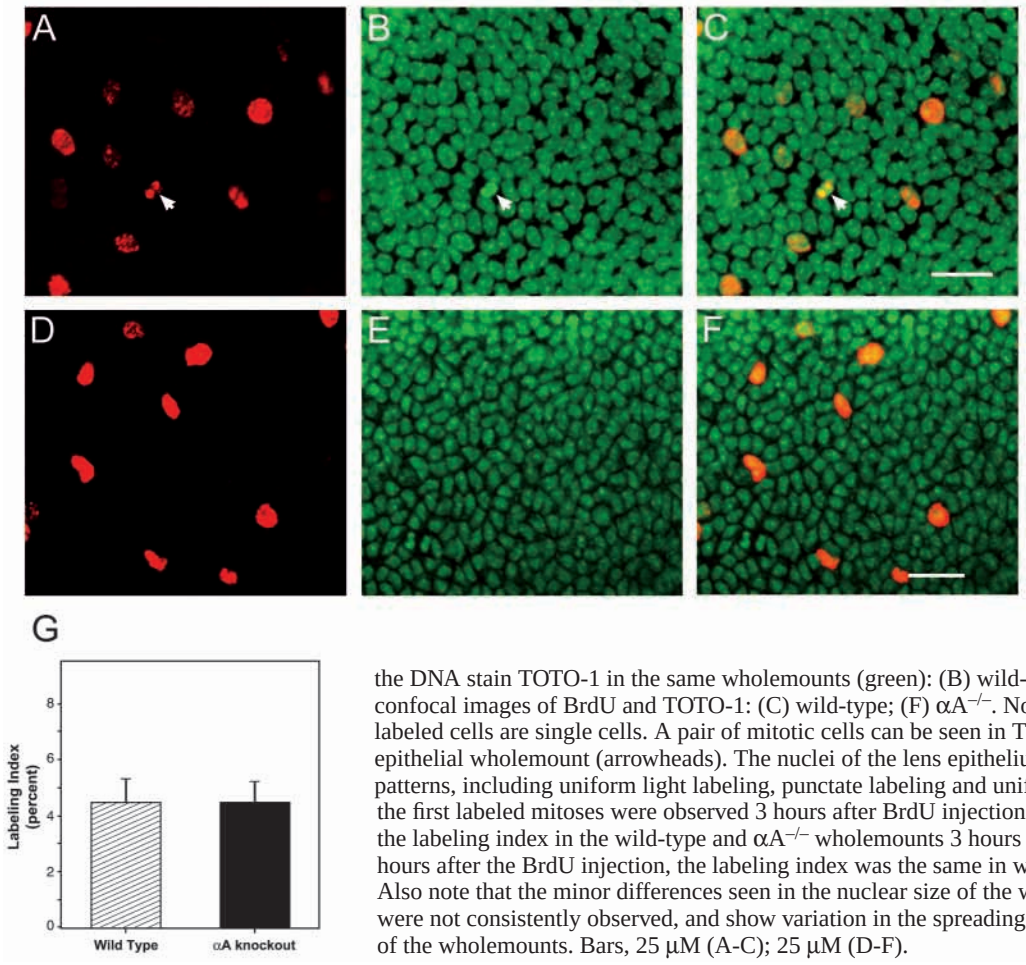

Fig. 2. Confocal micrographs of BrdU and TOTO-1 labeling in lens epithelial wholemounts 3 hours after injection of BrdU. Seven-day-old wild-type or $\alpha A^{-/-}$ mice were injected with BrdU and wholemounts of lens epithelium were fixed 3 hours after the BrdU injection. The chromosomes were stained with BrdU. (A,D) S-phase cells labeled with BrdU (red) in wild-type (A) or αA-knockout (D) lenses. (B,E) Cells labeled with the DNA stain TOTO-1 in the same wholemounts (green): (B) wild-type; (E), $\alpha A^{-/-}$. (C,F) Merged confocal images of BrdU and TOTO-1: (C) wild-type; (F) $\alpha A^{-/-}$. Note that the majority of the BrdU-labeled cells are single cells. A pair of mitotic cells can be seen in TOTO-1 staining of the wild-type epithelial wholemount (arrowheads). The nuclei of the lens epithelium demonstrate several staining patterns, including uniform light labeling, punctate labeling and uniform intense labeling. Note also that the first labeled mitoses were observed 3 hours after BrdU injection (A-C). (G) Quantitative analysis of the labeling index in the wild-type and $\alpha A^{-/-}$ wholemounts 3 hours after the BrdU pulse. Note that 3 hours after the BrdU injection, the labeling index was the same in wild-type and $\alpha A^{-/-}$ epithelial cells. Also note that the minor differences seen in the nuclear size of the wild-type and $\alpha A^{-/-}$ wholemounts were not consistently observed, and show variation in the spreading out and fixation during preparation of the wholemounts. Bars, 25 μM (A-C); 25 μM (D-F).

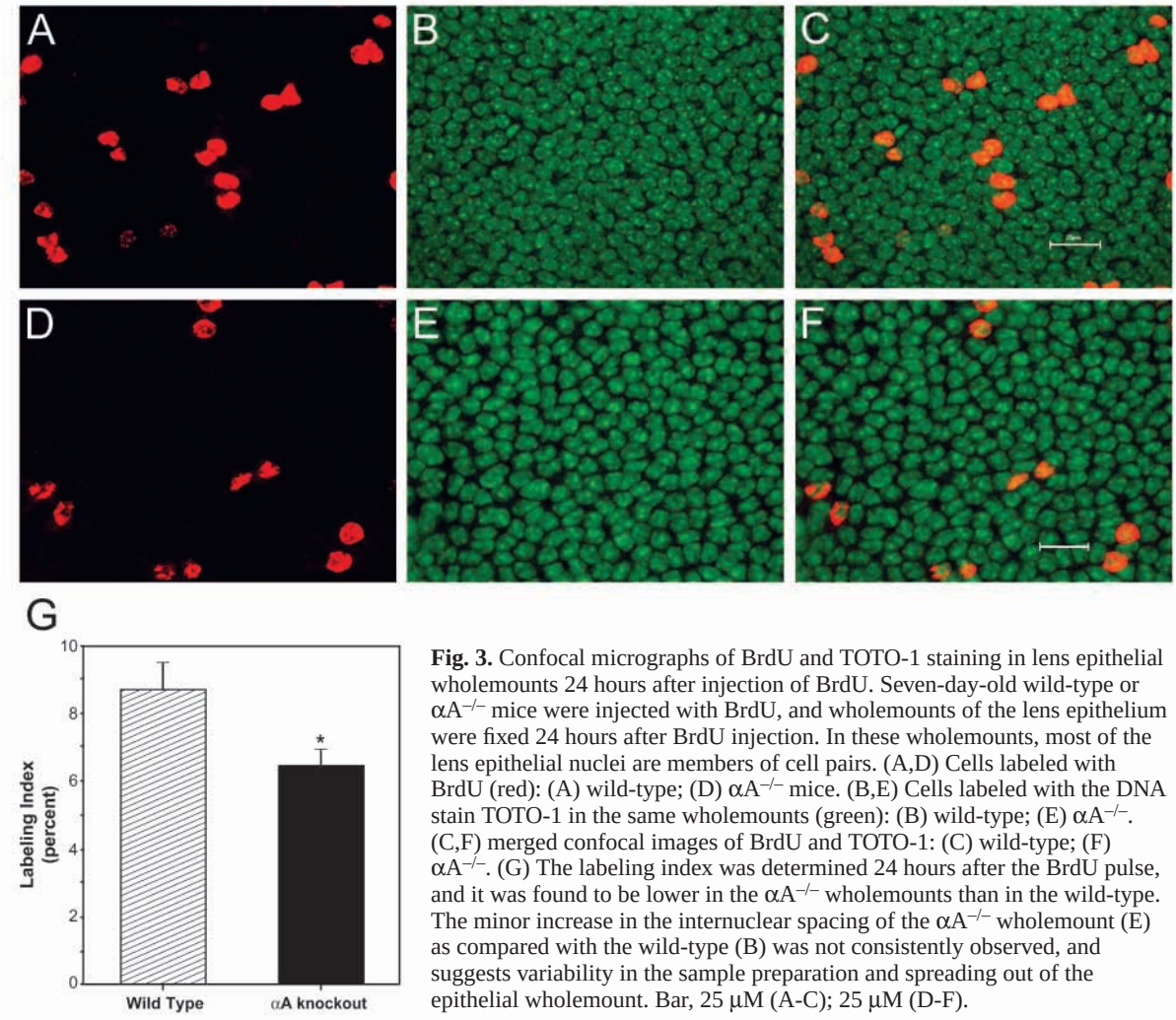

Fig. 3. Confocal micrographs of BrdU and TOTO-1 staining in lens epithelial wholemounts 24 hours after injection of BrdU. Seven-day-old wild-type or $\alpha A^{-/-}$ mice were injected with BrdU, and wholemounts of the lens epithelium were fixed 24 hours after BrdU injection. In these wholemounts, most of the lens epithelial nuclei are members of cell pairs. (A,D) Cells labeled with BrdU (red): (A) wild-type; (D) $\alpha A^{-/-}$ mice. (B,E) Cells labeled with the DNA stain TOTO-1 in the same wholemounts (green): (B) wild-type; (E) $\alpha A^{-/-}$. (C,F) merged confocal images of BrdU and TOTO-1: (C) wild-type; (F) $\alpha A^{-/-}$. (G) The labeling index was determined 24 hours after the BrdU pulse, and it was found to be lower in the $\alpha A^{-/-}$ wholemounts than in the wild-type. The minor increase in the internuclear spacing of the $\alpha A^{-/-}$ wholemount (E) as compared with the wild-type (B) was not consistently observed, and suggests variability in the sample preparation and spreading out of the epithelial wholemount. Bar, 25 μM (A-C); 25 μM (D-F).

BrdU-labeled cells. Thus, 24 hours after BrdU injection, all the BrdU-labeled nuclei in the lens epithelial wholemounts were in pairs (Fig. 3A-F). Both members of a cell pair had an identical staining pattern of their nuclei. The symmetrical pattern of BrdU staining in the daughter cells significantly assisted their identification as cell pairs. The labeling index of wild-type and $\alpha A^{-/-}$ lens epithelium was determined 24 hours after BrdU injection (Fig. 3G). The $\alpha A^{-/-}$ epithelium had fewer numbers of cell pairs compared with the wild-type epithelium. The 24-hour labeling index of the wild-type central epithelium doubled from 4.5±1.5 to 8.6±1.8% due to mitosis. In the epithelium of $\alpha A^{-/-}$ lenses, the 24-hour labeling index increased to 6.4±0.4% (from 4.5±1.3% at 3 hours), about 25% lower than wild-type lenses (n=18, P=0.008). This result suggests that only some of the cells were able to complete mitosis. The remainder did not complete mitosis, and presumably died during or soon after mitosis.

Pairs of BrdU-labeled cells remained close to each other for 2-5 days after the BrdU injection (Fig. 4B). The wild-type lenses gave us the baseline number of paired BrdU-labeled cells. The labeling index in the central region of wild-type and $\alpha A^{-/-}$ lens epithelial wholemounts at successive times after the BrdU pulse is shown in Fig. 5. We also divided the 24-hour time period after the BrdU injection into shorter intervals. The number of BrdU-labeled cells was counted after 1, 3, 8 and 16 hours in the wild-type and $\alpha A^{-/-}$ lens epithelial wholemounts. The labeling index was the same at 1-8 hours after the BrdU injection but, between 16 hours and 5 days after the BrdU injection (Fig. 5), the labeling index was significantly lower in the $\alpha A^{-/-}$ wholemounts compared with the wild-type. This result suggests that the lack of αA increased the susceptibility of both daughter cells to apoptosis.

We then looked for the number of single-labeled cells in the wild-type and $\alpha A^{-/-}$ lens epithelial explants 24 hours after the BrdU injection. If the number of single-labeled cells were more in the $\alpha A^{-/-}$ wholemount, it would mean that one of the two daughter cells formed in the $\alpha A^{-/-}$ epithelial wholemount had died, and would indicate that cell death occurred after cell division. The wild-type lenses gave us the baseline level of single-labeled cells. However, we found that a vast majority of BrdU-labeled cells were present as pairs in the lenses from both genotypes (Table 1). This suggests that the lack of αA increased the susceptibility of both daughter cells to apoptosis.

For each genotype, the labeling index did not change significantly between 1 and 3 days (Fig. 5). This indicates that the BrdU-labeled cells did not undergo a second division during this period. After 5 days, the labeling index in the central region

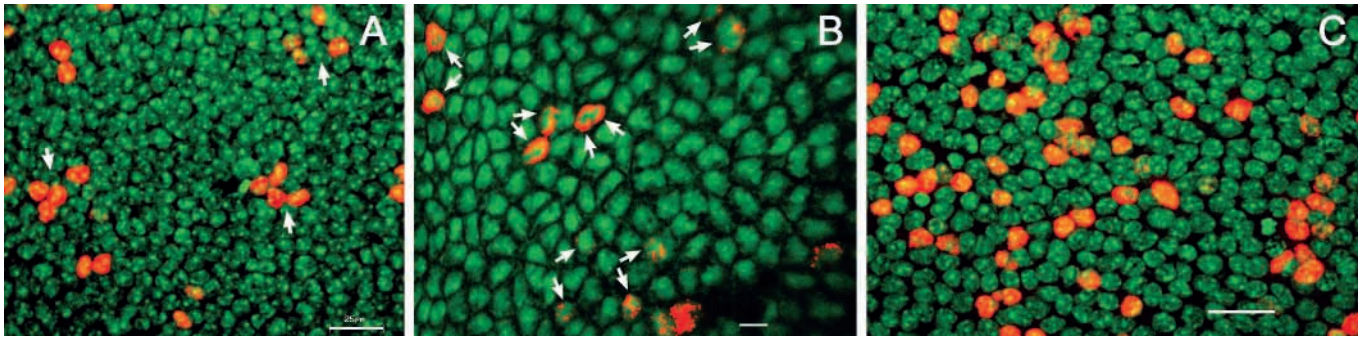

Fig. 4. Merged confocal micrographs of BrdU- and TOTO-1-stained nuclei in the lens epithelial wholemounts. (A) In this micrograph, several BrdU-labeled 'tetrads' can be seen (arrows) 24 hours after BrdU injection. Pairs of BrdU-labeled nuclei (red) were identified by their identical staining pattern. The wholemount was stained with TOTO-1 (green) to detect all the nuclei. Note that a majority of the nuclei were not labeled with BrdU. Bar, 25 μM. (B) BrdU and TOTO-1 staining in lens epithelial wholemounts 5 days after injection. Wild-type mice were injected with BrdU and wholemounts were fixed 5 days later. BrdU immunofluorescence (red) in the central region of the wholemount is shown. TOTO-1 (green) was used to label the nuclei of all the cells. Note that the BrdU-labeled cells were all members of cell pairs (arrows). Note also that, in some cases, members of a pair of BrdU-labeled nuclei were separated by two or more nuclei. Bar, 10 μM. (C) BrdU and TOTO-1 labeling in the periphery of a 7-day-old wild-type lens epithelial wholemount 24 hours after BrdU injection. Near the periphery (germinative region) of the lens epithelium, the labeling index was 2-3-fold higher as compared with the central region (Fig. 4A,B). In many cases, pairs of BrdU-labeled nuclei (red) that were very close to each other could be identified. In other cases, it was difficult to ascertain if two adjacent BrdU-labeled nuclei were members of a pair or not. TOTO-1 staining (green) was used to visualize all the nuclei. Bar, 25 μM.

decreased slightly, probably because the nonlabeled cells divided and therefore diluted the labeling index.

In a few cases, tetrads of BrdU-labeled nuclei were also seen 24 hours after the BrdU injection (Fig. 4A). The cell cycle normally lasts about 24 hours, and the S phase is about 6 hours, it is therefore unlikely that the tetrads arose from a second division of a pair of BrdU-labeled daughter cells. These tetrads most probably resulted from the mitotic division of two precursor daughter cells that were synchronized from a previous division, consistent with results of others (Rafferty and Rafferty, 1981).

In the peripheral region, the labeling index was 2-3-fold higher as compared with the central region and many of the pairs of labeled cell nuclei were immediately adjacent to other labeled pairs (Fig. 4C). This 'overcrowding' of the BrdU-labeled nuclei made it difficult to assess accurately whether adjacent BrdU-labeled nuclei were members of a pair or not. However, the labeling index in the peripheral region was determined to be 30% lower in the $\alpha A^{-/-}$ lens epithelial wholemounts than in the wild-type, confirming that the effects observed in the central region were also seen in the peripheral region of the epithelium.

During our examination of BrdU labeling in $\alpha A^{-/-}$ epithelial wholemounts, we made a significant observation. We observed cells in the $\alpha A^{-/-}$ epithelium that round up and shrink, thus losing intercellular contacts with neighboring cells (data not shown). These BrdU-labeled small cell debris resembled apoptotic bodies. The wholemounts were stained with TUNEL stain to determine whether the smaller nuclei represented dying cells. The lens epithelial wholemount of the $\alpha A^{-/-}$ lenses contained scattered pairs of apoptotic cells, and these were strongly labeled by the TUNEL assay (Fig. 6B,C). The labeled nuclei had a characteristic condensed morphology with small, positively labeled apoptotic bodies. These apoptotic bodies were often found in close association, and

Table 1. Percentage of BrdU-labeled cells that occur as pairs in the mouse lens epithelium

Time after BrdU injection	BrdU-labeled pairs in lens epithelial wholemount (%)	
	Wild-type	αA-knockout
3 hours	7.2	8.1
1 day	98.1	97.6
2 days	97.0	98.4
3 days	98.4	97.8
5 days	97.6	98.2

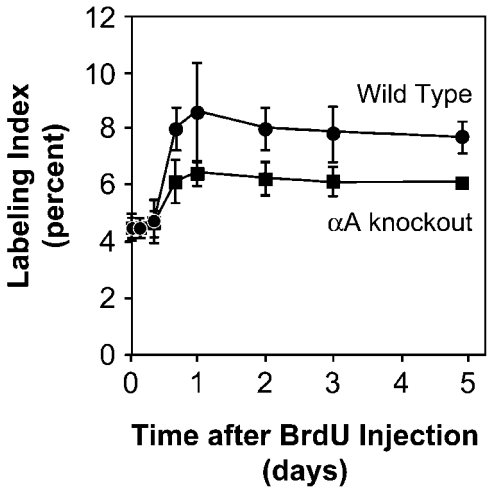

Fig. 5. BrdU labeling index in the lens epithelial wholemounts at successive times after BrdU injection. Seven-day-old wild-type or $\alpha A^{-/-}$ mice were injected with BrdU and wholemounts were fixed at successive times after the BrdU injection. The BrdU labeling index was determined at 1, 3, 8, 16 and 24 hours, and 2, 3 and 5 days after the BrdU injection. Four lenses were used at each time point. Note that the labeling index of the $\alpha A^{-/-}$ wholemount lagged the labeling index of the wild-type between 16 hours and 5 days.

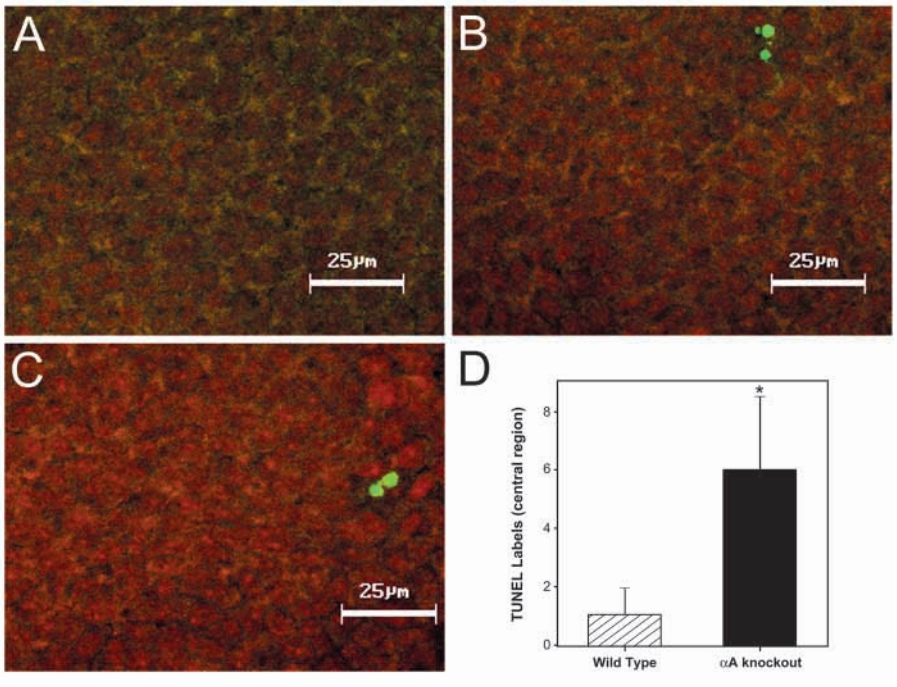

Fig. 6. Confocal micrographs of TUNEL staining in lens epithelial wholemounts. Seven-day-old mouse lens epithelial wholemounts were fixed and stained with the TUNEL staining kit. Propidium iodide was used to stain the DNA of all the nuclei in the wholemounts: (A) wild-type lens epithelium; (B,C) $\alpha A^{-/-}$ lens epithelium. In the wild-type wholemounts, TUNEL staining was rarely detected. Pairs of TUNEL-labeled cells (green) were scattered throughout the $\alpha A^{-/-}$ wholemounts. Note that the TUNEL-positive nuclei were nearly always seen as pairs. (D) Quantitative analyses of cell death in lens epithelial wholemounts. TUNEL-positive nuclei were counted in wild-type or $\alpha A^{-/-}$ lens epithelial wholemounts. In the wild-type lens epithelium, there was an average of one TUNEL stain in the central region. In the $\alpha A^{-/-}$ wholemount, there was an average of six TUNEL-stained nuclei. Data represent average of six wild-type and six $\alpha A^{-/-}$ wholemounts. Bars, 25 μM (A-C).

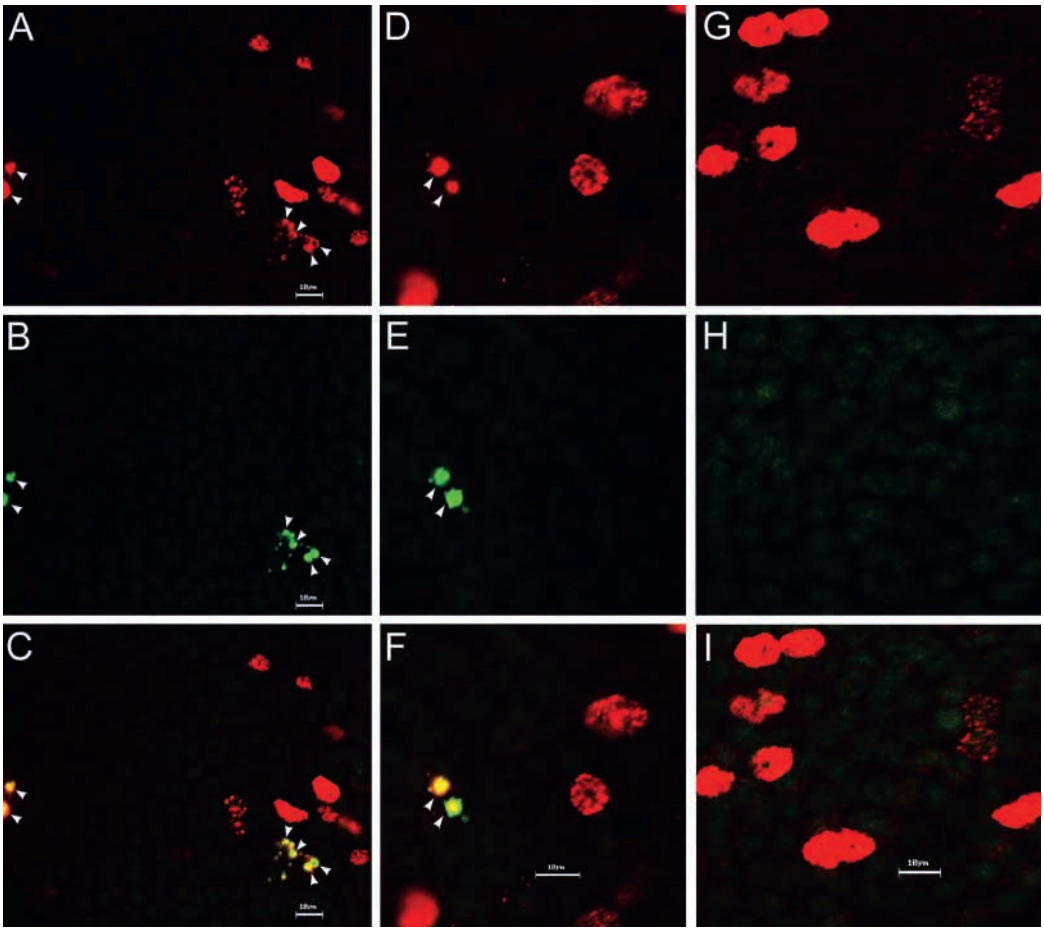

Fig. 7. Confocal images of TUNEL and BrdU staining in lens epithelial wholemounts. Seven-day-old wild-type and $\alpha A^{-/-}$ mice were injected with BrdU, and wholemounts were fixed 24 hours later. (A,D,G) BrdU-labeled cells. (B,E,H) TUNEL-labeled cells. (C,F,I) Merged confocal images of BrdU- and TUNEL-labeled cells in (A,D,G) and (B,E,H). In the $\alpha A^{-/-}$ lens epithelial wholemounts (A,D), several BrdU-labeled nuclei, smaller in size than normal, are scattered among the pairs of normal-sized BrdU-labeled nuclei. These smaller nuclei were often seen as distinct members of a pair (arrows). The smaller nuclei were intensely stained with TUNEL reagents (B,C,E,F). Note that the BrdU-labeled nuclei having normal dimensions were not stained with the TUNEL label. In the wild-type wholemounts, smaller BrdU-labeled nuclei were not detected often (G), and the TUNEL labeling was negligible (H,I). Bars, 10 μM (A-H).

appeared to be pairs of dying cells. In some cases, they appeared to be cleared by neighboring cells. The cellular debris or apoptotic bodies were frequently detected in the αA-knockout wholemounts, but were rarely detected in the wild-type epithelium (Fig. 6A,D).

To test whether BrdU-labeled cells were dying during

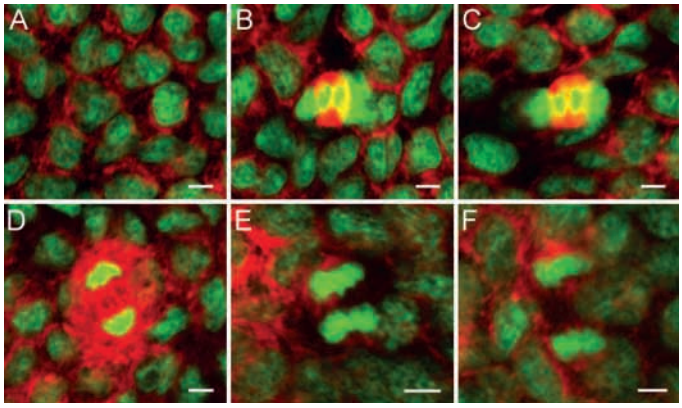

Fig. 8. Visualization of β-tubulin in lens epithelial wholemounts by immunofluorescence and confocal microscopy in different cell-cycle phases. Seven-day-old wild-type or $\alpha A^{-/-}$ mouse lens epithelial wholemounts were immunostained with an antibody to β-tubulin (red) and the nuclei were stained with TOTO-1 (green). (A) In the interphase of wild-type cells, β-tubulin was uniformly distributed around the nuclei. (B,C) In metaphase cells, the bundling of β-tubulin around the condensed chromosomes could be readily detected. Note that there was no difference in the organization of the metaphase spindles of the wild-type (B) and $\alpha A^{-/-}$ (C) lens epithelial wholemounts. (D-F) In anaphase cells of the wild-type epithelium, the spindle was well organized (D). However, there was disorganization of the anaphase spindle of the $\alpha A^{-/-}$ lens epithelial wholemounts (E,F). This aberrant spindle phenotype was observed in 45% of the anaphase spindles of the $\alpha A^{-/-}$ wholemounts. Twenty metaphase and 20 anaphase spindles in six different lens epithelial wholemounts were analyzed for each genotype. Bars, 5 μM.

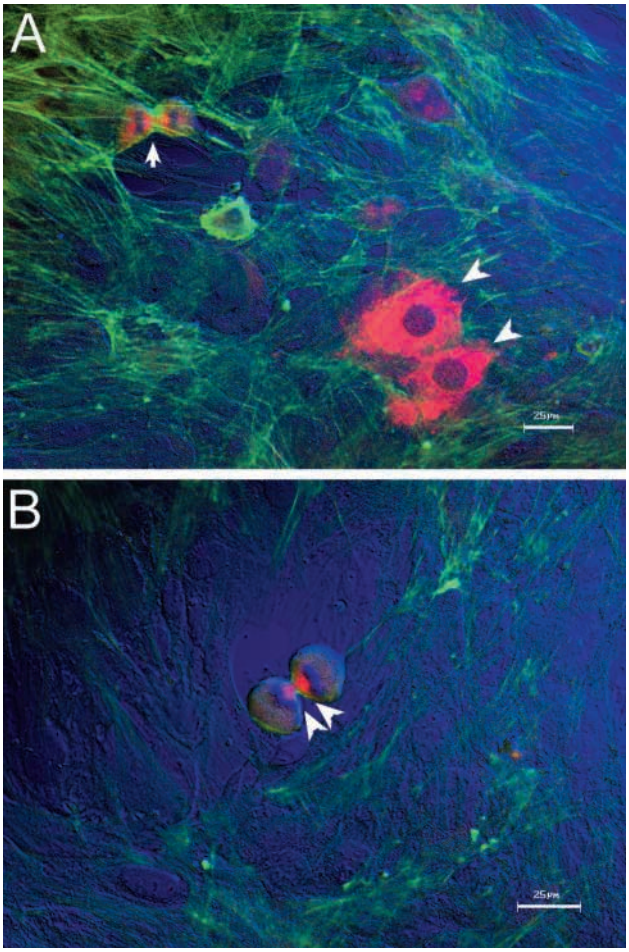

Fig. 9. Visualization of αA and F-actin in lens epithelial cells during mitosis. Merged confocal images of αA immunofluorescence (red) and F-actin staining (green) of wild-type mouse lens epithelial cells. Cell morphology was imaged with differential interference contrast (blue). (A) Cells in anaphase (arrow) or interphase (arrowheads). During interphase, αA was distributed throughout the cytoplasm. Note that a pair of recently divided cells remaining close to each other can be seen (arrowheads). (B) Cells in cytokinesis (arrowheads). Note that αA immunofluorescence (red) was concentrated in the middle of the dividing cells. Bars, 25 μm (A,B).

mitosis, dual staining with TUNEL reagents and BrdU antibodies was performed. Mice were injected with BrdU and, 24 hours later, the wholemounts were treated with TUNEL reagents first, and then immunostained to detect BrdU. Fig. 7 shows several closely spaced, BrdU-positive cells, which were also strongly stained by the TUNEL assay. These dying cells appeared to be in late stages of mitosis, probably in anaphase or cytokinesis since, in many cases, they appeared as pairs. We defined apoptotic cells as those cells whose nuclear diameter was a third or smaller than the size of a normal nucleus. The BrdU-labeled pairs that stained positively with the TUNEL reagents were a third or smaller than the size of the normal nuclei. By contrast, BrdU-labeled pairs that had normal dimensions were not stained by TUNEL reaction. These data suggest that the lower value of the labeling index in the $\alpha A^{-/-}$ lens epithelium may be due to an increase in apoptotic cell death during cell division.

αA and αB-crystallins have been shown to protect the cytoskeleton, and αB and several molecular chaperones are associated with the mitotic apparatus in dividing cells (Inaguma et al., 2001). Since the integrity of the spindle is essential for accurate cell division to occur, it is possible that cell death in lens epithelium lacking αA results from disorganization of the mitotic spindle. To examine the integrity of the mitotic spindle, wild-type and $\alpha A^{-/-}$ lens epithelial wholemounts were stained with an antibody to β-tubulin. Tubulin labeling was visualized by immunofluorescence and confocal microscopy. Fig. 8A shows that β-tubulin was uniformly stained around the nuclei of interphase cells. During metaphase, chromosome condensation and the bundling of microtubules in the metaphase spindle was readily detected (Fig. 8B,C). We examined 20 metaphase spindles each for the wild-type and $\alpha A^{-/-}$ lens epithelial wholemounts. There was no significant difference in the integrity of the metaphase spindle for the two genotypes.

We next examined the anaphase spindle of wild-type and $\alpha A^{-/-}$ lens epithelial wholemounts. Anaphase cells could be readily identified as pairs of cells with condensed chromosomes (Fig. 8D-F). In anaphase cells of wild-type wholemounts, well-developed arrays of microtubules nucleated from both the centrosomes, and were aligned between the separating chromosomes (Fig. 8D). However, in the $\alpha A^{-/-}$ wholemounts, there was a loss of astral microtubules, and microtubules in the zone between the chromosomes (Fig. 8E,F). We studied six wild-type and six $\alpha A^{-/-}$ wholemounts immunostained with the β-tubulin antibody. The integrity of

the spindle was examined in 20 pairs of anaphase cells for each genotype. The results showed that 95% of the anaphase spindles were well ordered in wild-type epithelium. However, 45% of the anaphase spindles of the $\alpha A^{-/-}$ lens epithelial wholemounts had a defective phenotype, suggesting that, in the absence of αA, the anaphase spindle is not well organized and that αA may play a role in maintaining the integrity of the microtubules in the lens epithelium.

To investigate the cellular distribution of αA in mitotic cells, wild-type mouse lens epithelial cells were cultured, and the primary cells were immunostained with antibody to αA. The cytoskeletal protein F-actin was stained with fluorescein phalloidin, and cellular morphology was imaged by differential interference contrast. These studies showed that αA was excluded from the chromosomes, but was highly concentrated in the middle of dividing cells (Fig. 9A,B). During interphase, αA was distributed uniformly throughout the cytoplasm (Fig. 9A).

To examine further whether αA may play a role in the integrity of the mitotic spindle, wild-type mouse lens epithelial cells were also double immunostained with αA and β-tubulin antibodies, to determine the distribution of αA in relation to the mitotic spindle. Fig. 10 shows the distribution of αA (green) and β-tubulin (red) in metaphase, anaphase and cytokinesis. These stages of mitosis were recognized by chromosome condensation using TOPRO-3 fluorescence (shown in blue). As can be seen in Fig. 10, αA immunofluorescence was excluded from the chromosomes of the dividing cells at all stages of mitosis. During metaphase, αA appears to be concentrated in the centrosomes of the mitotic spindle (Fig. 10A-C). However, the punctate staining pattern observed suggest that the microtubules are not necessarily the primary target of αA during early mitosis. During anaphase, αA was highly concentrated in the region between the chromosomes. However, significant punctate immunostaining for αA was also observed (Fig. 10E,F). This staining pattern suggests that αA associates with microtubules as well as with other cytoskeletal elements during anaphase. At cytokinesis, the intercellular bridge microtubules were labeled by the αA antibodies (Fig. 10H,I). At this stage, there appears to be a strong association with the

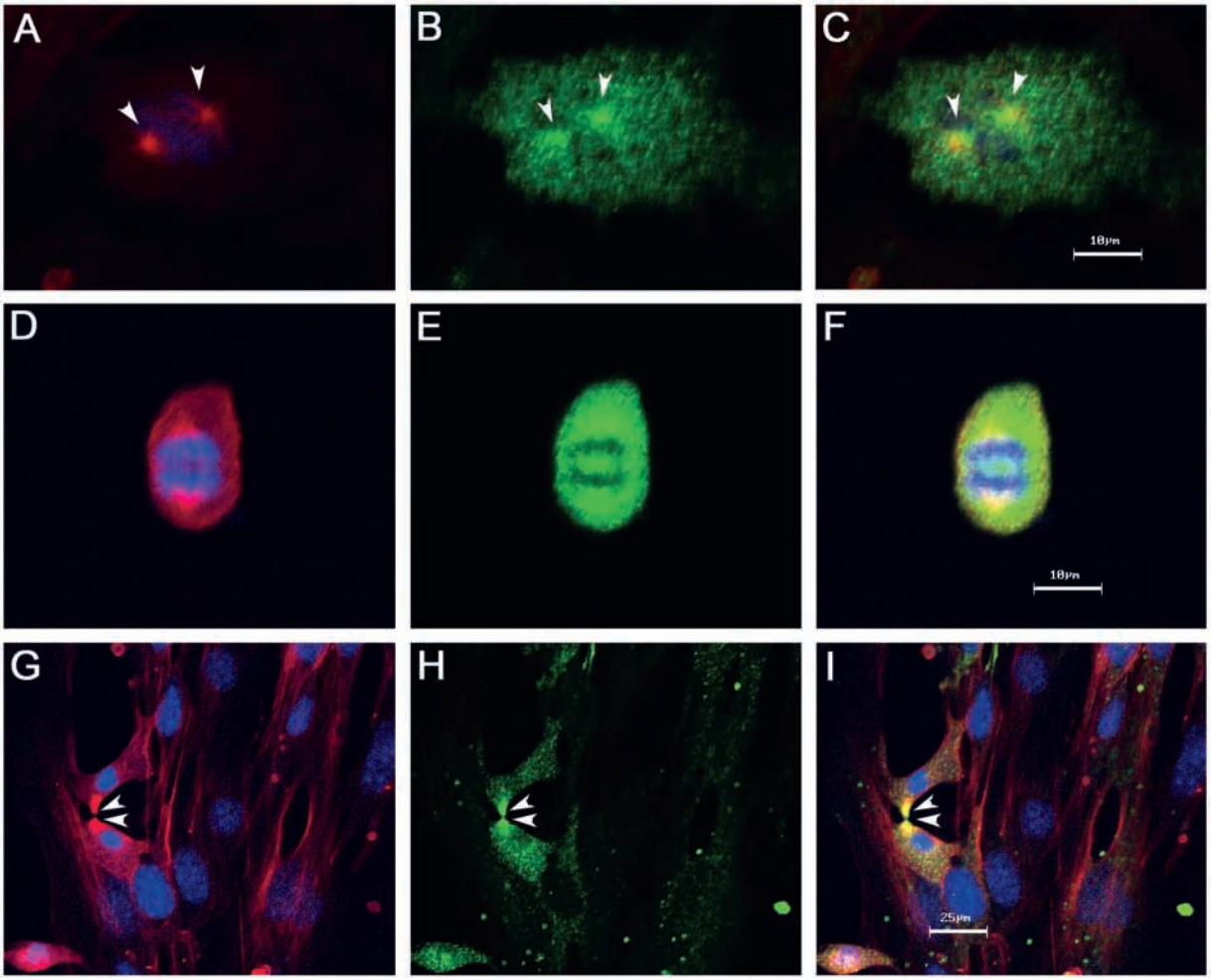

Fig. 10. Visualization of αA-crystallin and β-tubulin in lens epithelial cells during mitosis. Wild-type mouse lens epithelial cells were fixed and stained with anti-αA and an $Alexa^{488}$-conjugated secondary antibody (green). Cells were also immunostained with an antibody to β-tubulin and an $Alexa^{568}$-conjugated secondary antibody (red) and the nuclei were stained with TOPRO-3 (blue). (A-C) Metaphase, (D-F) anaphase and (G-I) cytokinesis. Note that αA was concentrated in the region of the centrosome in metaphase and in the intercellular bridge microtubules of the dividing cells during cytokinesis (arrowheads). Bars, 10 μm (A-F); 25 μm (G-I).

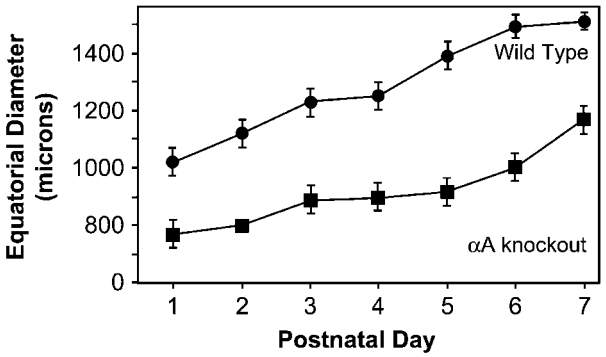

Fig. 11. Lens dimensions in wild-type and $\alpha A^{-/-}$ lenses. Mid-sagittal sections (4 μm) of wild-type and αA-knockout lenses were stained with hematoxylin and eosin. The lens sections were examined by confocal microscopy. The equatorial diameter of the lens was determined at different postnatal ages. The equatorial diameter of the $\alpha A^{-/-}$ lenses was ~30% smaller at birth and lagged in growth compared with the wild-type throughout the early postnatal period.

microtubule cytoskeleton, corroborating the results shown in Fig. 9B. These observations suggest that the relative distribution of αA is dependent upon the relative position of a cell during the cell cycle.

The αA-knockout mice had 40-50% smaller lenses in comparison with control mice, indicating that deletion of the gene encoding αA resulted in a lens growth deficiency. To determine when the growth deficiency became apparent, the size of the lenses was recorded as a function of age. The lens at postnatal day 0 was 40% smaller, and the growth lagged that of the control mice throughout the observation period (Fig. 11). The number of fiber cells could not be accurately determined because the 7-day-old αA-knockout lenses had disorganized fiber cell morphology in the central region of the lens.

To assess further if the smaller size of the $\alpha A^{-/-}$ lenses was due to smaller fiber cells, we examined the cross-sectional profiles in the periphery of the lenses using MIP immunofluorescence to visualize the fiber membranes. Lens slices (3 μm) were cut in the equatorial plane. Light microscopic analysis of the lenses indicated that the mean cross-sectional area of the secondary fiber cells in the cortex of the lens was 9.5±4.8 μm^2 for wild-type and 9.1±3.8 μm^2 for the $\alpha A^{-/-}$ (n=20, P=0.38). Although the cross-sectional profiles of the fiber cells appears to be indistinguishable for the wild-type and $\alpha A^{-/-}$ cells, since the wild-type lens is larger, its fiber cells are probably longer. However, the fiber cells of the wild-type and $\alpha A^{-/-}$ lenses had a distinctly altered organization, with fiber cell membranes being significantly smoother in the wild-type lens (Fig. 12). αA has been shown to associate with membranes (Boyle and Takemoto, 1996; Cobb and Petrash, 2000) and our studies suggest that it might affect the organization of the fiber cells. Taken together, these observations suggest that the reduced size of the $\alpha A^{-/-}$ lens is due to a reduction in the net production of epithelial cells, and hence the formation of fewer fiber cells.

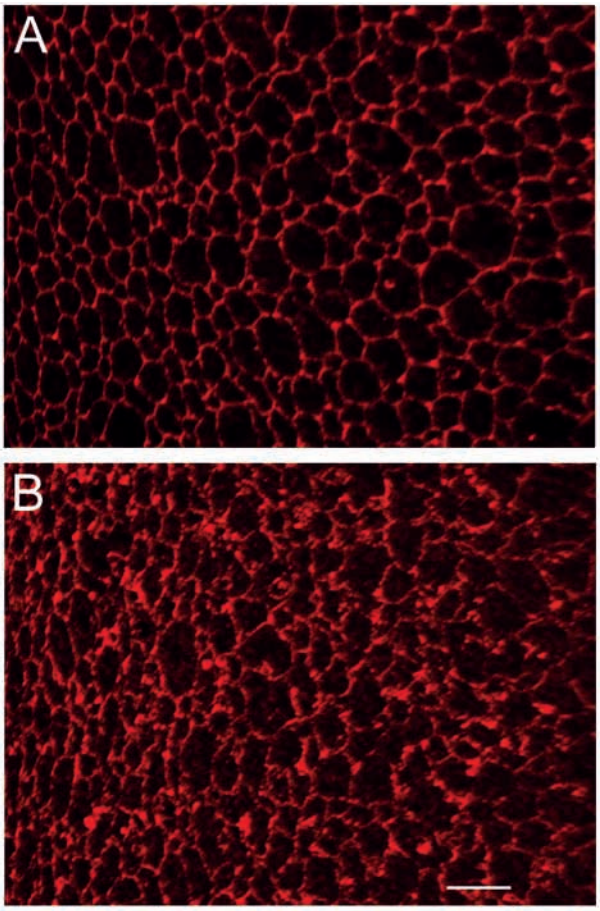

Fig. 12. Cross-sectional area of fiber cells in wild-type and $\alpha A^{-/-}$ mouse lenses. Lens slices were cut in the equatorial plane and stained with an antibody to MIP (AQP0) to visualize fiber cell membranes. The distance from the center of the lens was 300 μm. The organization of the fiber cells in these equatorial sections of wild-type and $\alpha A^{-/-}$ mice is different, and the membranes of the wild-type lens fiber cells appear smoother than those of the $\alpha A^{-/-}$. Variation in the cross-sectional areas of the different fiber cells was noted for both wild-type and $\alpha A^{-/-}$ cells. However, the distribution of the cross-sectional areas of the fiber cells was similar in wild-type and $\alpha A^{-/-}$ lenses. Bar, 10 μM (A,B).

Discussion

In this study, we tested the hypothesis that αA prevents cell death at a specific stage of the cell cycle in vivo in the mouse lens epithelium. By labeling S-phase cells in wild-type and $\alpha A^{-/-}$ mice in vivo, and by following the fate of the cells as they proceed through the G_2 to M and post-mitotic stages, we have identified the phase of the cell cycle at which αA most likely prevents cell death. This method allowed us to obtain detailed information about the effect of αA expression on cell-cycle progression. Our data indicate that there were fewer BrdU-labeled cells 24 hours after BrdU injection in the $\alpha A^{-/-}$ lens epithelium than in the wild-type. This means that some cells were dying in the $\alpha A^{-/-}$ lens epithelium, around the time of mitosis. Our data further show that αA expression had no effect on the labeling of cells in the S phase, or in the S to G_2 transition, or during G_2, or in G_2 to M transition. This is because, if cells were dying during the above-mentioned phases, we would have observed an increase in the percentage of single, BrdU-labeled cells. We did not observe an increase in the percentage of single-BrdU-labeled cells (Table 1). This

indicates that pairs of daughter cells died in the absence of αA during cell division. These data combined with the TUNEL labeling of pairs of BrdU-labeled mitotic cells not only eliminate a cell death during other cell-cycle phases, but also suggest that the lack of αA may be associated with mitotic cell death during anaphase or cytokinesis. Moreover, the $\alpha A^{-/-}$ lens epithelial wholemounts did not have a higher number of single BrdU-labeled cells 2, 3 or 5 days after the pulse than at 24 hours, arguing against the likelihood that cells were dying post-mitosis in the absence of αA. Our data strongly suggest that cells die as pairs, and supports the idea that cell death probably occurs during the late stages of mitosis.

It is also possible that only one of the two daughter cells died soon after mitosis in the $\alpha A^{-/-}$ wholemount. In this case, we would have observed single BrdU-labeled cells 24 hours after the BrdU pulse. However, the absence of single BrdU-labeled cells 24 hours after the pulse in the αA-knockout wholemounts argues against this possibility. Overall, the data suggest that the lack of αA increased the susceptibility of both daughter cells to apoptosis.

Although the emphasis in this study has been on the central region of the 7-day-old lens epithelial wholemounts, similar effects of the lack of αA were seen in the germinative and central region. The labeling index in the peripheral (germinative) region was also determined to be 30% lower in the $\alpha A^{-/-}$ lens epithelial wholemounts than in the wild-type, confirming that the effects observed in the central region were also seen in the peripheral region of the epithelium. However, due to overcrowding of the BrdU-labeled nuclei in this region, we were unable to ascertain whether the labeled nuclei were members of a pair.

Deletion of the gene encoding αA results in an increased light scattering in the fiber cells in the central region of 7-week-old mouse lenses (Brady et al., 1997). In older mice, the entire lens becomes opaque. The increased light scattering is due to the formation of inclusion bodies within the interior fiber cells of the αA-knockout lens. The inclusion bodies primarily comprise αB and HSP25, two other members of the small HSP family that can form co-aggregates with αA. The presence of these inclusion bodies has been taken as an indication that αA is necessary for maintaining the solubility of αB and HSP25. Others have also shown that the 7-week-old $\alpha A^{-/-}$ lens is smaller than the wild-type (Brady et al., 1997). We confirmed and extended this finding in this study and showed that the growth defect in the $\alpha A^{-/-}$ lenses occurred early in life. Lenses of newborn mice were 40% smaller and continued to lag in growth throughout early postnatal life. It had not been investigated in earlier studies whether the lens is smaller because of fewer fiber cells or smaller fiber cells (due to loss of a major cytoplasmic protein). The current work suggests that, during cell division in vivo, only some of the $\alpha A^{-/-}$ cells were able to produce daughter cells, and the others died during or soon after completing mitosis.

The hypothesis that cells were dying during mitosis is supported by our observations that there were more TUNEL-positive cells in the $\alpha A^{-/-}$ lens epithelial wholemounts, and these TUNEL-positive cells often appeared as pairs. These dying cells were considerably reduced in size. Furthermore, our studies revealed that BrdU-labeled cells similar in appearance to apoptotic bodies were detected more frequently in the $\alpha A^{-/-}$ lens epithelium than in the controls. These apoptotic bodies also strongly stained with the TUNEL stain, and were almost always found in pairs, suggesting that the lack of αA increased the susceptibility of both daughter cells to apoptosis.

The present results suggest that αA may act at the checkpoint that controls the exit of cells from mitosis. The exit of cells from mitosis is controlled by checkpoints that monitor the assembly and position of the mitotic spindle. Cells defective in assembly of the mitotic spindle produce abnormal cells that die by apoptosis (Paulovich et al., 1997; Karsenti and Vernos, 2001). Cell death associated with mitosis has been observed in a few experimental systems (Chen et al., 2002). Cells can also arrest in mitosis when the microtubule spindle assembly is disrupted, with drugs such as nocodazole (Lanni and Jacks, 1998). The mitotic spindle performs several well-documented functions, including the capture and segregation of the duplicated parental chromosomes to daughter cells (Shimoda and Soloman, 2002; Heald, 2000). The central spindle is required for cell cleavage (Glotzer, 1997) and the essential components of the central spindle required for cytokinesis have been identified (Mishima et al., 2002). Our studies showed that the anaphase spindle of $\alpha A^{-/-}$ cells was not properly assembled in a significant proportion of mitotic cells, and suggest that $\alpha A^{-/-}$ cells died at mitosis in anaphase or cytokinesis. This points to a role of the spindle assembly in the apoptotic cell death in this study.

The current work showed that, during mitosis in mouse lens epithelial cells, the distribution of αA increased around the centrosomes during metaphase. However, additional punctate staining patterns observed (Fig. 10B,C) suggest that the microtubules are not necessarily a main target of αA during early mitosis. αA was excluded from the chromosomes of dividing cells, but continued to be expressed at a high level around the chromosomes, and in the middle of the cell during anaphase. This staining pattern suggests that αA probably associates with the microtubules as well as other cytoskeletal elements. At cytokinesis, the intercellular bridge microtubules were strongly labeled by the αA antibodies. At this stage, there appeared to be a strong association with the microtubule cytoskeleton (Fig. 10H,I). αA is redistributed into the cytoplasm during interphase (Fig. 9A). These observations suggest that the relative distribution of αA is dependent upon the relative position of a cell in the cycle. Interestingly, a recent study showed that a phosphorylated form of αB is associated with centrosomes and midbodies during cytokinesis (Inaguma et al., 2001). It is possible that αA, a closely related protein, may also be involved with the quality control of proteins such as tubulin, a major component of the mitotic spindle. Such a role for αA would be consistent with the importance of small HSPs in organization of different elements of the cytoskeleton such as the intermediate filaments and actin (Nicholl and Quinlan, 1994; Perng et al., 1999; Head and Goldman, 2000), and by its association with actin (Gopalakrishnan and Takemoto, 1992; Fitzgerald and Graham, 1991). αB has also been suggested to be a chaperone for tubulin (Arai and Atomi, 1997; Liang and MacRae, 1997; Leroux et al., 1997). The hypothesis that αA may play a role in cell division in the lens epithelium is supported by findings that molecular chaperones are involved in various aspects of cell growth and differentiation (Yokota et al., 1999; Wigley et al., 1999; Inaguma et al., 2001; Brown et al., 1996; Dunn et

al., 2001). Studies on synchronized cells in primary cultures are necessary to identify further the cell-cycle stage at which αA is involved.

αA is expressed very early during lens development (Robinson and Overbeek, 1996). Our studies suggest that αA may play a role in preventing apoptosis in vivo. During eye development, apoptosis is morphologically documented in the very early stages of lens vesicle formation (Garcia-Porrero et al., 1984; Ishizaki et al., 1993), is thought to play a role in primary or secondary fiber cell maturation and denucleation (Bassnett and Mataic, 1997; Bassnett, 2002), and may be associated with differentiation of lens epithelial cells into fibers in the rat lens (Ishizaki et al., 1998). A recent study suggests that the addition of αA to lens epithelial cells induces differentiation (Boyle and Takemoto, 2000). Aberrant proliferation and apoptosis occurs in vivo in transgenic mouse lenses expressing the polyoma large T antigen, and in the developing lenses of Rb-deficient mice (Griep et al., 1993; Morgenbesser et al., 1994). Cell-cycle entry and cell death has been reported in post-mitotic lens fiber cells by overexpression of E2F (Chen et al., 2000). Apoptosis does not seem to play a major role in age-related cataract formation (Harocopos et al., 1998). Small HSPs regulate programmed cell death (Arrigo, 2000; Kamradt et al., 2001; Paul et al., 2002). It is not yet known whether the cell death that we have observed occurs by p53-dependent mechanisms, although p53 expression has been documented in the murine lens epithelium (Pokroy et al., 2002). Additional studies will be necessary to investigate the possible role of αA during embryonic growth of the lens.

The present study raises new and important questions about the function of αA in the lens and in other tissues. The expression of αA and αB in nonlenticular tissues, their in vitro properties such as their autokinase activity (Kantorow and Piatigorsky, 1994), interaction with cytoskeletal elements (Quinlan, 2002), and the ability to protect cells from stress-induced apoptosis (Andley et al., 1998), suggest that these proteins have general cellular functions. Further studies in cultured cells are needed to ascertain whether the expression of αA directly alters the cell cycle.

In summary, we have demonstrated that $\alpha A^{-/-}$ lenses undergo slower proliferation and higher apoptosis in vivo than the wild-type controls. Moreover, our data suggest that αA expression protects lens epithelial cells in vivo from apoptotic cell death associated with mitosis. These results are consistent with the observed protective phenotype conferred by αA expression in vitro in cultured lens epithelial cells (Andley et al., 1998; Andley et al., 2000). It is interesting to note that, in contrast to the slower growth observed in $\alpha A^{-/-}$ lens epithelial cells, the absence of αB, the aggregation partner of αA in the lens, enhances the frequency of hyperproliferation and tetraploidy in cultured lens epithelial cells, suggesting a cell-cycle-associated role of αB (Andley et al., 2001). Further studies are necessary to investigate whether the mitosis-associated cell death that we have observed in the $\alpha A^{-/-}$ lens epithelium occurs by a p53-dependent mechanism in vivo. The system used here can serve as a useful model for future studies.

We are indebted to E. Wawrousek (National Eye Institute, NIH) for providing the $\alpha A^{-/-}$ mice. We are grateful to D. Beebe for many helpful discussions throughout this work. We also thank S. Bassnett for helpful discussions and for critical comments on the manuscript. We thank P. Fitzgerald for providing the monoclonal antibody to αA-crystallin. This work is supported by National Eye Institutes grants R01EY05681 (U.P.A.), core grant EY02687 and Research to Prevent Blindness.

References

Andley, U. P., Song, Z., Wawrousek, E. F. and Bassnett, S. (1998). The molecular chaperone αA-crystallin enhances lens epithelial cell growth and resistance to UVA stress. *J. Biol. Chem.* **273**, 31252-31261.

Andley, U. P., Song, Z., Wawrousek, E. F., Fleming, T. P. and Bassnett, S. (2000). Differential protective activity of αA and αB-crystallins in lens epithelial cells. *J. Biol. Chem.* **275**, 36823-36831.

Andley, U. P., Song, Z., Wawrousek, E. F., Brady, J. P., Bassnett, S. and Fleming, T. P. (2001). Lens epithelial cells derived from αB-crystallin knockout mice demonstrate hyperproliferation and genomic instability. *FASEB J.* **15**, 221-229.

Arai, H. and Atomi, Y. (1997). Chaperone activity of alpha B-crystallin suppresses tubulin aggregation through complex formation. *Cell Struct. Funct.* **22**, 539-544.

Arrigo, A. P. (2000). sHsp as novel regulators of programmed cell death and tumorigenicity. *Pathol. Biol.* **48**, 280-288.

Bassnett, S. (2002). Lens organelle degradation. *Exp. Eye Res.* **74**, 1-6.

Bassnett, S. and Mataic, D. (1997). Chromatin degradation in differentiating fiber cells of the eye lens. *J. Cell Biol.* **137**, 27-49.

Beebe, D. C. and Masters, B. R. (1996). Cell lineage and the differentiation of corneal epithelial cells. *Invest. Ophthalmol. Vis. Sci.* **37**, 1815-1825.

Bhat, S. P. and Nagineni, C. N. (1989). αB subunit of lens-specific protein α-crystallin is present in other ocular and non-ocular tissues. *Biochem. Biophys. Res. Commun.* **158**, 319-325.

Bhat, S. P., Hale, I. L., Matsumoto, B. and Elghanayan, D. (1999). Ectopic expression of αB-crystallin in Chinese hamster ovary cells suggests a nuclear role for this protein. *Eur. J. Cell Biol.* **78**, 143-150.

Boyle, D. L. and Takemoto, L. J. (1996). EM immunolocalization of alpha-crystallins: association with the plasma membrane from normal and cataractous human lenses. *Curr. Eye Res.* **15**, 577-582.

Boyle, D. L. and Takemoto, L. (2000). A possible role for α-crystallins in lens epithelial cell differentiation. *Mol. Vis.* **6**, 63-71.

Brady, J. P., Garland, D., Douglas-Tabor, Y., Robison, W. G., Jr, Groome, A. and Wawrousek, E. F. (1997). Targeted disruption of the mouse αA-crystallin gene induces cataract and cytoplasmic inclusion bodies. *Proc. Natl. Acad. Sci. USA* **94**, 884-889.

Brady, J. P., Garland, D., Green, D. E., Tamm, E. R., Giblin, F. J. and Wawrousek, E. F. (2001). αB-crystallin in lens development and muscle integrity: a gene knockout approach. *Invest. Ophthalmol. Vis. Sci.* **42**, 2924-2934.

Brown, C. R., Doxey, S. J., Hong-Brown, L. O., Martin, R. L. and Welch, W. J. (1996). Molecular chaperones and the centrosome. A role for TCP-1 in microtubule nucleation. *J. Biol. Chem.* **271**, 824-832.

Chen, Q., Huang, F. C., Fromm, L. and Overbeek, P. A. (2000). Induction of cell cycle entry and cell death in postmitotic lens fiber cells by overexpresion of E2F1 or E2F2. *Invest. Ophthalmol. Vis. Sci.* **41**, 4223-4231.

Chen, Q. M., Merrett, J. B., Dilley, T. and Purdom, S. (2002). Down-regulation of p53 with HPV E6 delays and modifies cell death in oxidant response of human diploid fibroblasts: an apoptosis-like cell death associated with mitosis. *Oncogene* **21**, 5313-5324.

Cobb, B. A. and Petrash, J. M. (2000). Characterization of alpha-crystallin-plasma membrane binding. *J. Biol. Chem.* **275**, 6664-6672.

deFazio, A., Leary, J., Hedley, D. and Tattersall, M. (1987). Immunohistochemical detection of proliferating cells in vivo. *J. Histochem. Cytochem.* **35**, 571-577.

de Jong, W. W., Leunissen, J. A. M. and Voorter, C. E. M. (1993). Evolution of the α-crystallin/small heat shock protein family. *Mol. Biol. Evol.* **10**, 103-126.

Djabali, K., Piron, G., de Nechaud, B. and Portier, M. M. (1999). αB-crystallin interacts with cytoplasmic intermediate filament bundles during mitosis. *Exp. Cell Res.* **253**, 649-662.

Dunn, A. Y., Melville, M. W. and Frydman, J. (2001). Review: cellular substrates of the eukaryotic chaperonin TRiC/CCT. *J. Struct. Biol.* **135**, 176-184.

Fitzgerald, P. and Graham, D. (1991). Ultrastructural localization of alpha

A-crystallin to the bovine lens fiber cytoskeleton. *Curr. Eye Res*. **10**, 417-436.

Garcia-Porrero, J. A., Colvee, E. and Ojeda, J. L. (1984). The mechanism of cell death and phagocytosis in early chick lens morphogenesis: a scanning electron microscopy and cytochemical approach. *Anat. Rec*. **208**, 123-136.

Glotzer, M. (1997). The mechanism and control of cytokinesis. *Curr. Opin. Cell Biol*. **9**, 815-823.

Gopalakrishnan, S. and Takemoto, L. (1992). Binding of actin to lens alpha-crystallins. *Curr. Eye Res.* **11**, 929-933.

Griep, A. E., Herbert, R., Jeon, S., Lohse, J. K., Dubielzig, R. R. and Lambert, P. F. (1993). Tumorigenicity by human papilloma virus type 16 E6 and E7 in transgenic mice correlates with alterations in epithelial cell growth and differentiation. *J. Virol*. **67**, 1373-1384.

Harocopos, G. J., Alvares, K. M., Kolker, A. E. and Beebe, D. C. (1998). Human age-related cataract and lens epithelial cell death. *Invest. Ophthalmol. Vis. Sci*. **39**, 2696-2706.

Head, M. W. and Goldman, J. E. (2000). Small heat shock proteins, the cytoskeleton, and inclusion body formation. *Neuropathol. Appl. Neurobiol*. **26**, 304-312.

Heald, R. (2000). Motor functions in the mitotic spindle. *Cell* **102**, 399-402.

Horwitz, J. (1992). The function of α-crystallins. *Proc. Natl. Acad. Sci. USA* **89**, 10449-10453.

Horwitz, J. (2000). The function of alpha-crystallin in vision. *Semin. Cell Dev. Biol*. **11**, 53-60.

Hyatt, G. A. and Beebe, D. C. (1985). Regulation of lens cell growth and polarity by an embryo-specific growth factor and by inhibitors of lens cell proliferation and differentiation. *Development* **117**, 701-709.

Inaguma, Y., Ito, H., Iwamoto, I., Saga, S. and Kato, K. (2001). αB-crystallin phosphorylated at Ser-59 is located in centrosomes and midbodies during mitosis. *Eur. J. Cell Biol.* **80**, 741-748.

Ishizaki, Y., Voyvodic, J. T., Burne, J. F. and Raff, M. C. (1993). Control of lens epithelial cell survival. *J. Cell Biol.* **121**, 899-908.

Ishizaki, Y., Jacobson, M. D. and Raff, M. (1998). A role for caspases in lens differentiation. *J. Cell Biol.* **140**, 153-158.

Kamradt, M. C., Chen, F. and Cryns, V. L. (2001). The small heat shock protein αB-crystallin negatively regulates cytochrome c- and caspase-8-dependent activation of caspase-3 by inhibiting its autoproteolytic maturation. *J. Biol. Chem*. **276**, 16059-16063.

Kantorow, M. and Piatigorsky, J. (1994). α-Crystallin/small heat shock protein has autokinase activity. *Proc. Natl. Acad. Sci. USA* **91**, 3112-3116.

Karsenti, E. and Vernos, I. (2001). The mitotic spindle: A self-made machine. *Science* **294**, 543-547.

Kuszak, J. R., Clark, J. I., Cooper, K. E. and Rae, J. L. (2000). Biology of the lens: Lens transparency as a function of embryology, anatomy, and pathology. In *Principles and Practice of Ophthalmology*, Vol. 2, 2nd edn (ed. D. M. Albert and F. A. Jakobiec), Chapter 100, pp. 1355-14085. Philadelphia: W. B. Saunders.

Lanni, J. S. and Jacks, T. (1998). Characterization of the p53-dependent post-mitotic checkpoint following spindle disruption. *Mol. Cell. Biol*. **18**, 1055-1064.

Leroux, M. R., Melki, R., Gordon, B., Batelier, G. and Candido, P. M. (1997). Structure-function studies on small heat shock protein oligomeric assembly and interaction with unfolded peptides. *J. Biol. Chem*. **272**, 24646-24656.

Liang, P. and MacRae, T. H. (1997). Molecular chaperones and the cytoskeleton. *J. Cell Sci*. **110**, 1431-1440.

Litt, M., Kramer, R., LaMorticella, D. M., Murphey, W., Louvrien, E. W. and Weleber, R. G. (1998). Autosomal dominant congenital cataract associated with a missense mutation in the human alpha crystalline gene *CRYAA*. *Hum. Mol. Genet.* **7**, 471-474.

McAvoy, J. W. and Chamberlain, C. G. (1989). Fibroblast growth factor induces different responses in lens epithelial cells depending on its concentration. *Development* **107**, 221-228.

Mehlen, P., Mehlen, A., Godet, J. and Arrigo, A. P. (1997). hsp27 as a switch between differentiation and apoptosis in murine embryonic fibroblasts. *J. Biol. Chem*. **272**, 31657-31665.

Mikulicich, A. G. and Young, R. W. (1963). Cell proliferation and displacement in the lens epithelium of young rats injected with tritiated thymidine. *Invest. Ophthalmol*. **2**, 344-354.

Mishima, M., Kaitna, S. and Glotzer, M. (2002). Central spindle assembly and cytokinesis requires a kinesin-like protein/RhoGAP complex with microtubule bundle activity. *Dev. Cell* **2**, 41-54.

Morgenbesser, S. D., Williams, B. O., Jacks, T. and DePinho, R. A. (1994). p53-dependent apoptosis produced by Rb-deficiency in the developing mouse lens. *Nature* **371**, 72-74.

Nicholl, I. D. and Quinlan, R. A. (1994). Chaperone activity of alpha-crystallins modulates intermediate filament assembly. *EMBO J.* **13**, 945-953.

Paul, C., Manero, F., Gonin, S., Kretz-Remy, C., Virot, S. and Arrigo, A. P. (2002). Hsp27 as a negative regulator of cytochrome c release. *Mol. Cell. Biol*. **22**, 816-834.

Paulovich, A. G., Toczyski, D. P. and Hartwell, L. H. (1997). When checkpoints fail. *Cell* **88**, 315-321.

Perng, M. D., Cairns, L., van den Ijssel, P., Prescott, A., Hutcheson, A. M. and Quinlan, R. A. (1999). Intermediate filament interactions can be altered by HSP27 and αB-crystallin. *J. Cell Sci.* **112**, 2099-2112.

Pokroy, R., Tendler, Y., Pollack, A., Zinder, O. and Weisinger, G. (2002). p53 expression in the normal murine eye. *Invest. Ophthalmol. Vis. Sci*. **43**, 1736-1741.

Quinlan, R. (2002). Cytoskeletal competence requires molecular chaperones. *Prog. Mol. Biol. Subcellular Biol*. **28**, 219-233.

Rafferty, N. S. and Rafferty, K. A. (1981). Cell population kinetics of the mouse lens epithelium. *J. Cell. Physiol.* **107**, 309-315.

Rakic, J. M., Galand, A. and Vrensen, G. F. (1997). Separation of fibers from the capsule enhances mitotic activity of human lens epithelium. *Exp. Eye Res*. **64**, 67-72.

Reddan, J. R. (1982). Control of cell division in the ocular lens, retina and vitreous. In *Cell Biology of the Eye* (ed. D. McDevitt), pp. 299-275. New York: Academic Press.

Robinson, M. L. and Overbeek, P. A. (1996). Differential expression of alpha A- and alpha B-crystallin during murine ocular development. *Invest. Ophthalmol. Vis. Sci.* **37**, 2276-2284.

Sax, C. and Piatigorsky, J. (1994). Expression of the α-crystallin/small heat-shock protein/molecular chaperone gene in the lens and other tissues. *Adv. Enzymol. Relat. Areas Mol. Biol.* **69**, 155-201.

Shimoda, S. L. and Soloman, F. (2002). Integrating functions at the kinetochore. *Cell* **109**, 9-12.

Singh, D. P., Ohguro, N., Kikuchi, T., Sueno, T., Reddy, V. N., Yuge, K., Chylack, L. T. and Shinohara, T. (2000). Lens epithelium derived growth factor LEDGF: Effects on growth and survival of lens epithelial cells, keratinocytes and fibroblasts. *Biochem. Biophys. Res. Commun.* **267**, 371-381.

Srinivasan, A. N., Nagineni, C. N. and Bhat, S. P. (1992). alpha A-crystallin is expressed in non-ocular tissues. *J. Biol. Chem*. **267**, 23337-23341.

Vicart, P., Caron, A., Guicheney, P., Li, Z., Prevost, M.-C., Faure, A., Chateau, D., Chapon, F., Tome, F., Dupret, J.-M. et al. (1998). A missense mutation in the αB-crystallin chaperone gene causes a desmin-related myopathy. *Nat. Gen.* **20**, 92-95.

Wigley, W. C., Fabunmi, R. P., Lee, M. G., Marino, C. R., Muallem, S., DeMartino, G. N. and Thomas, P. J. (1999). Dynamic association of proteasomal machinery with the centrosomes. *J. Cell Biol*. **145**, 481-490.

Yokota, S., Yanagi, H., Yura, T. and Kubota, H. (1999). Cytosolic chaperonin is up-regulated during cell growth. Preferential expression and binding to tubulin at G_1/S transition through early S phase. *J. Biol. Chem.* **274**, 37070-37078.

Zelenka, P. S., Gao, C. Y., Rampalli, A., Aurora, J., Chauthwale, V. and He, H. Y. (1997). Cell cycle regulation in the lens: proliferation, quiescence, apoptosis and differentiation. *Prog. Retinal Eye Res.* **16**, 303-322.